

To Appear in the Astrophysical Journal Letters

Cometary Astropause of Mira Revealed in the Far-Infrared

Toshiya Ueta

Department of Physics and Astronomy, University of Denver, Denver, CO 80208

tueta@du.edu

ABSTRACT

Evolved mass-losing stars such as Mira enrich the interstellar medium (ISM) significantly by their dust-rich molecular wind. When these stars move fast enough relative to the ISM, the interaction between the wind and ISM generates the structure known as the astropause (a stellar analog of the heliopause), which is a cometary stellar wind cavity bounded by the contact discontinuity surface between the wind and ISM. Far-infrared observations of Mira spatially resolve the structure of its astropause for the first time, distinguishing the contact surface between Mira's wind and the ISM and the termination shock due to Mira's wind colliding with the ISM. The physical size of the astropause and the estimated speed of the termination shock suggest the age of the astropause to be about 40,000 yr, confirming a theoretical prediction of the shock re-establishment time after Mira has entered the Local Bubble.

Subject headings: circumstellar matter — infrared: stars — stars: AGB and post-AGB — stars: individual (Mira) — stars: mass loss

1. Introduction

Mira is the archetype of asymptotic giant branch (AGB) stars, which contribute significantly to the enrichment of the interstellar medium (ISM) by a dust-rich molecular stellar wind (e.g. Sedlmayr 1994). Hence, tracing mass-loss histories of these stars has a profound impact on knowledge of the composition of the ISM and its evolution in host galaxies. Mira is actually a wind-accreting binary system (Reimers & Cassatella 1985): a mass-losing AGB star is the primary star (Mira A), dominating the system. Mira's wind is, therefore, a cool molecular wind from the primary, in which dust grains convert radiation pressure of the star into the outward momentum of the wind (Kwok 1975; Steffen, Szczerba, & Schöberner 1998).

Previous investigations in CO line emission revealed that Mira's wind at $\sim 4 \text{ km s}^{-1}$ formed a circumbinary molecular envelope of 0.3 in radius, whose otherwise spherical structure was punctuated by bipolar outflows at $\sim 8 \text{ km s}^{-1}$ (Josselin et al. 2000; Fong et al. 2006). Mira's space velocity is approximately 150 km s^{-1} nearly due south as calculated via a spherical trigonometric transformation (Johnson & Soderblom 1987) using its proper motion (Perryman et al. 1997), radial velocity (Evans 1967) and the solar motion (Dehnen & Binney 1998).

Hence, Mira's wind has been interacting with the ISM flow local to Mira for quite some time. This interaction left a turbulent wake of approximately 2 degrees long, observed in emission in the ultraviolet (Martin et al. 2007) and 21 cm H I line (Matthews et al. 2008). The ultraviolet emission is thought to be

due to H_2 excited collisionally by hot electrons arising from the shocked ISM flow. The 21 cm line emission of atomic hydrogen is, therefore, expected from dissociation of H_2 into H.

This is the second case of the wind-ISM interaction around an AGB star after R Hya, in which a bow shock resulting from the interaction was seen in the far-infrared (Ueta et al. 2006). While the $\text{H}_2/\text{H I}$ wake of Mira has been attributed to the wind-ISM interaction owing to Mira’s large space velocity, distinct shock layers of the interaction themselves have not been confirmed observationally, except for the possible bow shock structure seen in the ultraviolet (Martin et al. 2007). Thus, it has been unclear how the $\text{H}_2/\text{H I}$ turbulent wake seen at the large spatial scale is physically related to the CO wind seen at the small spatial scale, except that bright H_2 streams (Martin et al. 2007) are correlated spatially with CO bipolar outflows (Josselin et al. 2000).

In this letter, we present Mira’s far-infrared image taken with the *Spitzer Space Telescope* (*Spitzer*; Werner et al. 2004), which resolves spatially the structure of Mira’s astropause (a stellar analog of the heliopause; Neusch & Fahr 1982) for the first time. Resolved are (1) Mira’s circumbinary dust envelope at the core of the astropause, (2) the termination shock where the stellar wind is slowed down by the ISM and (3) the astrosheath in which a turbulent wake assumes the characteristic cometary shape beyond the termination shock. Thus, the *Spitzer* $160\mu\text{m}$ data, in conjunction with previous multi-wavelength results, provide the most comprehensive view of the wind-ISM interaction for an AGB star to date.

2. Observations and Data Reduction

Mira happened to be located at the northern edge of the XMM-LSS field in the *Spitzer* Wide-Area Infrared Extragalactic Legacy Survey (SWIRE; Lonsdale et al. 2003). Far-infrared mapping of Mira and its vicinity was performed on 2004 August 1 and 2 with the Multiband Imaging Photometer for *Spitzer* (MIPS; Rieke et al. 2004). Due to the relative position offset among the MIPS detectors in the focal plane, Mira was scanned over only in the 24 and $160\mu\text{m}$ bands (scans 08 and 09; AOR KEYs 5844992, 5845248, 11774976 and 11775232). These scans were done at the medium rate along five scan legs of 3° long each with a cross-scan stepping of $148''$. Quick inspection of the archived data indicated that Mira was saturated in both of the 24 and $160\mu\text{m}$ bands: however, the $160\mu\text{m}$ data appeared salvageable.

Data reduction was done in the following steps with the Ge Reprocessing Tools (GeRT; ver. 20060415 of S14 processing)¹ and the the Mosaicker software (ver. 20070615).² First, we used GeRT to create our own basic calibrated data (BCD). Bright sources can corrupt stimulator-response calibration if they happen to be on the detector when the calibrating stimulator is illuminated (Gordon et al. 2005). Thus, we excluded stimulator frames affected by bright Mira to optimize the time-dependent detector responsivity calibration for our particular data set. We also adjusted the number of reads in the data ramp to recover valid data in otherwise saturated pixels. Then, we applied a high-pass time median filter with a 50-detector-pixel width on the custom-made BCDs to remove the “streakings” due to residual slow-response variations of the detector, while masking out a circular region around Mira of 30-detector-pixel radius to avoid filtering out the extended structure around Mira. Finally, the custom-processed BCDs were mosaicked into a single map with the Mosaicker.

¹Available from <http://ssc.spitzer.caltech.edu/mips/gert/>.

²Available from <http://ssc.spitzer.caltech.edu/postbcd/>.

The MIPS $160\mu\text{m}$ band is known to suffer from a short-wavelength light leak, which can result in a false point source offset from the position of the true $160\mu\text{m}$ source (Gordon et al. 2005). Inspection of the mosaicked Mira map indicated that the emission core was elongated by the presence of a secondary point source offset from Mira (Figure 1a). Since Mira’s J magnitude is -0.7 (more than 6 magnitudes above the limit over which the leak becomes detectable), the core elongation was most likely due to the leak. Hence, we removed the light leak in the Mira map by scaling and subtracting the image of a calibration K2III star, HD 163588, whose $160\mu\text{m}$ emission was known to be mostly the leak³. This yielded a single-peaked, PSF-like emission core. This method would inevitably subtract the photospheric component of HD 163588 (estimated to be 56 mJy) from Mira. However, it was deemed negligible with respect to the flux of Mira at $160\mu\text{m}$ (52 Jy).

3. Results and Discussion

Figure 1 displays versions of the *Spitzer*/MIPS image of Mira at $160\mu\text{m}$ in log-scaled false-color. These maps were made at the $12''.0 \text{ pix}^{-1}$ scale ($11''.7 \times 13''.3$ field of view) with the mean sky coverage of $3.5 \pm 1.9 \text{ pixel}^{-1}$. The effect of saturation was not removed entirely by adjusting reads in the data ramp, and the $12''.0 \text{ pix}^{-1}$ scale turned out to be the minimum pixel scale for which all pixels register valid data. The one σ sensitivity and the average large-spatial-scale sky emission (the component removed during the median filter) were found to be 0.8 and $8.8 \pm 1.0 \text{ MJy sr}^{-1}$, respectively. The derived sky emission value was consistent with the estimated value of 6.5 MJy sr^{-1} , which is obtained with the *Spitzer* Planning Observations Tool (SPOT) software.⁴ Contours are 80, 60, 40, 20, 10, 5, 2.5 and 0.5% of the emission peak, with the lowest contour corresponding to 3σ ($= 2.5 \text{ MJy sr}^{-1}$).

The light-leak-corrected image is presented in Figure 1b, in which the emission core is evidently single-peaked. The leak-corrected emission profile of Mira can be dissected into three distinct emission regions: the emission core, plateau and halo. The core is slightly extended with the full-width at half-maximum (FWHM) of $1''.0 \times 0''.9$ at the position angle (PA; measured East from North) of 70° . Since nearby point sources have the average FWHM of $0''.7$, the extension of the core appears genuine. The plateau is an elliptical region ($3''.4 \times 2''.8$ at the PA of 70°) of relatively flat profile encircling the core (at 5% to 30% of the peak emission). The halo is a fainter nebulosity surrounding the plateau. If we define the periphery of the halo at 3σ (the lowest contour in Figure 1), then its extent is $8''.5 \times 6''.5$ at the PA of 15° . The scan-map direction is the PA of 160° , along which some residual “streakings” are still recognizable below 3σ . Hence, the elongation of the $160\mu\text{m}$ emission around Mira is not the artifact of scan mapping. Mira has been imaged in the far-IR most recently with the *AKARI Infrared Astronomy Satellite* (Murakami et al. 2007). *AKARI*’s Mira maps are consistent with the *Spitzer* map with a single-peaked emission core with extension at the PA of 15° (H. Izumiura et al. 2008, private communication).

The point-spread-function (PSF) in the MIPS $160\mu\text{m}$ band has the first Airy pattern out to $\sim 7'$ (at $12'' \text{ pixel}^{-1}$) at $\sim 4\%$ of the peak surface brightness. A synthesized PSF⁵ was convolved with an elliptical Gaussian function to conform the observed shape of the core and subtracted from the data (Figure 1c). We immediately see that there is still substantial emission ($\sim 50 \text{ MJy sr}^{-1} = \sim 20\sigma$) in the plateau, suggesting

³MIPS Data Handbook Ver. 3.3.1 (<http://ssc.spitzer.caltech.edu/mips/dh/>), p.76.

⁴<http://ssc.spitzer.caltech.edu/documents/background/>

⁵Available at <http://ssc.spitzer.caltech.edu/archanal/contributed/stinytim/>.

that it is caused by an elliptical ring of $2'.4 \times 2'.0$ at the PA of 70° . The core is oriented in the same way as the circumbinary CO envelope (Josselin et al. 2000), while the CO envelope is smaller than the core (Fong et al. 2006). At the distance of 107 pc to Mira (Knapp et al. 2003), the physical size of the CO envelope is $\sim 3 \times 10^{16}$ cm in radius. This agrees well with the expected radius of Mira’s molecular envelope resulted from mass loss at the rate of $\sim 2 \times 10^7 M_\odot \text{ yr}^{-1}$ (Josselin et al. 2000; Ryde & Schöier 2001; Fong et al. 2006), including the effect of photodissociation by the interstellar radiation field (Mamon, Glassgold, & Huggins 1988). Therefore, the core represents Mira’s circumbinary dust envelope whose physical size is $\sim 4.5 \times 10^{16}$ cm in radius.

Since the Mira system is moving at $\sim 150 \text{ km s}^{-1}$ the resulting wind-ISM interaction has given rise to the ultraviolet bow shock structure (Martin et al. 2007), despite Mira’s slow wind velocity of 4 km s^{-1} (Josselin et al. 2000; Fong et al. 2006). Figures 2a and 2b clearly show that the downstream side of the ultraviolet bow shock coincides with the southern edge of the far-infrared halo. Moreover, the cometary shape of the halo is the most consistent with the bow shock interpretation, in which the far-infrared nebulosity is shaped by a turbulent wake flowing almost due north. According to the theory of the (solar)wind-ISM interaction, the ISM flow approaches supersonically toward Mira, becomes subsonic past the bow shock and streams around the astropause, while Mira’s wind expands freely to form a bubble bounded by the termination shock, beyond which the wind becomes compressed and turbulent and flows downstream in the astrosheath (Zank 1999). Assuming that the $160\mu\text{m}$ emission probes Mira’s dusty wind emanating from the circumbinary envelope, we interpret that the leak-corrected, core-subtracted image distinguishes spatially all components of the astropause (Figure 1c) with the halo tracing the astrosheath and the emission ring delineating the termination shock (see, also, Figure 2d).

The prominent ultraviolet streams (Figures 2a and 2b) are outflows of H_2 excited collisionally by hot electrons in the bow-shock-excited ISM flow (Martin et al. 2007). These H_2 flows, therefore, must have penetrated the termination shock and been directed downstream while getting excited in the astrosheath. In the astrosheath, H_2 can be dissociated by either the interstellar radiation field (Mamon, Glassgold, & Huggins 1988) or collisional excitation (Martin et al. 2007; Matthews et al. 2008). The observed H I emission is mostly concentrated in the vicinity of the termination shock, with the peak FWHM of $1'.8$ (Matthews et al. 2008), which is compatible with the size of the molecular radius given the resolution at 21 cm (Figure 2c). Similar to H_2 , atomic H is directed toward downstream beyond the termination shock, lending strong support for the multi-phase characteristics of the flow in the astrosheath.

The stagnation point of the wind-ISM interaction is therefore at the apex of the halo (astropause), which is 3.6×10^{17} cm from Mira. Requiring ram pressure balance at the stagnation point, this implies that the ISM density local to Mira is $n_{\text{ISM}} = 0.02 \text{ cm}^{-3}$. This value is consistent with the result of a two-wind model (Wareing et al. 2007) that accounts for Mira’s entry into the Local Bubble, the region of warm ($\sim 10^6$ K), tenuous ($\sim 0.01 \text{ cm}^{-3}$) ISM in the solar neighborhood (Lallement 2001). Given $N_{\text{HI}} \leq 1.3 \times 10^{19} \text{ cm}^{-2}$ and 25% abundance of neutral species (Matthews et al. 2008), we can estimate the optical depth at $160\mu\text{m}$ to be 8×10^{-6} assuming a power-index scaling law with the index of 1.2 (i.e. silicate dust). Under the assumption that thermal dust emission dominates at $160\mu\text{m}$, the emission map and the optical depth yield the temperature of dust; $\sim 500 - 1100$ K in the circumbinary dust envelope, ~ 200 K in the termination shock and $\sim 30 - 200$ K in the astrosheath.

Based on these estimates, the pre-shock temperature of Mira’s wind is thought to be ~ 50 K (assuming gas-dust thermalization), implying Mach number of 7.5. With the generalized jump relations (e.g. Petelski 1981), the velocity of the termination shock is -2 km s^{-1} in Mira’s frame and the ratio of post- to pre-shock densities 3.8. These values yield the post-shock gas temperature of ~ 900 K. Thus, in the shock-excited

astrosheath, dust is still present (the gas temperature is below the condensation temperature of silicates ≈ 1200 K; Salpeter 1977), but probably de-thermalized from gas. Spectroscopic follow-ups are necessary to investigate the evolution of the dust-gas characteristics upon passage of the termination shock.

At 2 km s^{-1} , the termination shock should have taken $\sim 40,000$ yr to advance to the present position ($1 \times 10^{17} \text{ cm}$) from the astropause ($3.6 \times 10^{17} \text{ cm}$). The total flux of the astrosheath (including the termination shock) is 37 Jy, and this translates to the total mass of $7 \times 10^{-3} M_{\odot}$ using the dust emissivity of generic interstellar dust (Draine & Li 2007). With Mira’s mass loss rate ($\sim 2 \times 10^{-7} M_{\odot} \text{ yr}^{-1}$; Josselin et al. 2000; Fong et al. 2006; Ryde & Schöier 2001)⁶, it should have taken $\sim 40,000$ yr for the astrosheath to form. These estimates for the age of the termination shock is consistent with the time needed for the termination shock to re-establish itself after entering the Local Bubble ($\sim 40,000$ yr) as estimated numerically by Wareing et al. (2007), who attributed a kink in Mira’s ultraviolet tail (Martin et al. 2007) to Mira’s entry into the Local Bubble.

The presence of the bow shock indicates that the outer shock is supersonic. In the warm ($\sim 10^6$ K), tenuous ($\sim 0.01 \text{ cm}^{-3}$) Local Bubble (Lallement 2001), however, the shock velocity of $\sim 150 \text{ km s}^{-1}$ is barely supersonic. This suggests that the pre- and post-shock parameters across the bow shock are nearly continuous. This is consistent with the fact that the ultraviolet emission profile does not indicate any density enhancement (i.e. material pile-up) at the southern edge of the bow. Hence, ultraviolet emission in front of the upstream face of the astropause is due to excitation of the post-shock ISM gas by a shear flow. While Mira’s wind and the ISM gas flow are in general separated by the astropause, these flows are inherently turbulent. Thus, these flows are mixed in the downstream wake and H_2 is collisionally excited, resulting in the observed far-ultraviolet emission. Excited H_2 can be dissociated, leading to the observed H I emission. Dust grains help H_2 to replenish in the wake, and this cool, turbulent three-phase gas flow results in emission of H_2 and H I continuing at least for 1.5° long.

Hence, there is an emerging picture of Mira’s astropause (Figure 2d). The extent of the far-infrared emission outlines the astropause, which is the contact surface between Mira’s molecular wind and the ISM flow. The bulk of the halo emission is due to dusty molecular wind material in the astrosheath, shock-excited by the termination shock delineated by the emission ring. The termination shock is the discontinuous interface between the pre- and post-shock regions of Mira’s wind, inside which Mira’s wind expands undisturbed coming off the circumbinary envelope hosting bipolar outflows.

Since the post-shock regions of both Mira’s wind and the ISM flow have a significant physical size, the shock must be non-radiative (i.e., it has not been cooled down and compressed into an unresolvable size). According to Ferland et al. (1998), in a collisionally excited solar wind abundance gas heating dominates cooling below 10^4 K (their Fig. 6). The estimated post-shock gas temperature of Mira’s wind is ~ 900 K. Thus, the post-shock gas can indeed maintain its temperature, i.e., its physical size. Because previous numerical models (Wareing et al. 2007; Raga et al. 2008) were concerned mainly with the structure of the turbulent wake of the wind-ISM interaction, follow-up multi-phase hydrodynamical modeling at low temperatures to reproduce the structure of the astropause appears extremely worthwhile.

The total flux of the astropause is 52 Jy, which implies the total mass of $1 \times 10^{-2} M_{\odot}$ using the dust emissivity of generic interstellar dust (Draine & Li 2007). Since the total atomic mass in the astropause is $1.3 \times 10^{-3} M_{\odot}$ (Matthews et al. 2008), the total molecular mass is estimate to be $8.7 \times 10^{-3} M_{\odot}$ to be roughly

⁶Various authors quote a range of mass-loss rates for Mira, which is a variable star. In the present paper, however, we are concerned with the long-term effects of Mira’s mass loss. Therefore, we adopt the average rate of mass loss in our discussion.

1 to 9 atomic-to-molecular mass ratio. The observed far-ultraviolet luminosity implies the H_2 dissociation rate of $\sim 2.5 \times 10^{42} \text{ s}^{-1}$, if collisional excitation accounts for all far-ultraviolet emission (Martin et al. 2007). This rate, however, would have yielded a factor of four more atomic H than observed (Matthews et al. 2008). Dust grains can potentially provide H_2 formation sites to reduce excess atomic H. Using parameters of gas in the astrosheath ($n_{\text{H}} \approx 7$ and $T_{\text{gas}} \approx 900 \text{ K}$) and silicate grains ($0.1 \mu\text{m}$ radius, 3.7 g cc^{-1} , 1% mass ratio), the H_2 formation rate is approximately $4 \times 10^{40} \text{ s}^{-1}$, if one assumes that an encounter with two atomic H by a dust grain always results in production of H_2 . This suggests that H_2 far-ultraviolet emission is not entirely due to collision of H_2 with hot electrons and by some other means as already implied (Martin et al. 2007; Matthews et al. 2008) and/or there exist some mechanisms to bolster production of H_2 from atomic H.

Clearly, Mira’s astropause presents a unique laboratory for investigations of a multi-phase hydrodynamical flow, turbulence and dust-gas processing, which has a profound impact on the chemical makeup of the ISM. Because recent findings suggest that wind-ISM interaction around AGB stars may be common (Ueta et al. 2006, 2007), spatially resolved spectroscopy of multi-phase dusty, low-temperature gas flow will be extremely productive in the coming era of Herschel, SOFIA and ALMA (e.g. Pilbratt et al. 2003; Becklin, Tielens, & Callis 2007; Olofsson 2008, respectively).

Ueta thanks T. Le Bertre and L. D. Matthews for making their H I data available and R. E. Stencel for careful reading of the manuscript. This work is based on archival data obtained with the Spitzer Space Telescope, which is operated by the Jet Propulsion Laboratory, California Institute of Technology under a contract with NASA. Support for this work was provided partially by an award issued to the University of Denver by JPL/Caltech.

REFERENCES

- Becklin, E. E., Tielens, A. G. G. M., & Callis, H. H. S. 2007, *Adv. Space Res.* 40, 644
- Dehnen, W., & Binney, J. J. 1998, *MNRAS*, 298, 387
- Draine, B., & Li, A. 2007, *ApJ*, 657, 810
- Evans, D. S. 1967, in *Proc. IAU Symp. 30, Determination of Radial Velocities and their Applications*, eds. A. H. Batten, & J. F. Heard (Academic Press, London), 57
- Ferland, G. J., Korista, K. T., Verner, D. A., Ferguson, J. W., Kingdon, J. B., & Verner, E. M. 1998, *PASP*, 110, 761
- Fong, D., Meixner, M., Sutton, E. C., Zalucha, A., & Welch, W. J. 2006, *ApJ*, 652, 1626
- Gordon, K. D., et al. 2005, *PASP*, 117, 503
- Johnson, D. R. H., & Soderblom, D. R. 1987, *AJ*, 93, 864
- Josselin, E., Maun, N., Planesas, P., & Bachiller, R. 2000, *A&A*, 362, 255
- Knapp, G. R., Pourbaix, D., Platais, I., & Jorissen, A. 2003, *A&A*, 403, 993
- Kwok, S. 1975, *ApJ*, 198, 583
- Lallement, R. 2001, *Sp. Sci.* 277, 205

- Lonsdale, C. J., et al. 2003, *PASP*, 115, 897
- Martin, D. C., et al. 2007, *Nature*, 448, 780
- Matthews, L. D., Libert, Y., Gérard, E., Le Bertre, T., & Reid, M. J. 2008, *ApJ*, 684, 603
- Mamon, G. A., Glassgold, A. E., & Huggins, P. J. 1988, *ApJ*, 328, 797
- Murakami, H., et al. 2007, *PASJ*, 59, 369
- Neutsch, W., & Fahr, H. J. 1982, *MNRAS*, 202, 735
- Olofsson, H. 2008, *Astrophys. Space Sci.* 313, 201
- Perryman, M. A. C., et al. 1997, *A&A*, 323, L49
- Petelski, E. F. 1981, *J. Geophys. Res.* 86, 4803
- Pilbratt, G. L., et al. 2003, *Proc. SPIE* 4850, 586
- Raga, A. C., Cantó, J., De Colle, F., Esquivel, A., Kajdic, P., Rodríguez-González, A., Velázquez, P. F. 2008, *ApJ*, in press (astro-ph/0805.0549)
- Reimers, D., & Cassatella, A. 1985, *ApJ*, 297, 275
- Rieke, G., et al. 2004, *ApJS*, 154, 25
- Ryde, N., & Schöier, F. L. 2001, *ApJ*, 548, 384
- Salpeter, E. E. 1977, *ARA&A*, 15, 267
- Sedlmayr, E. 1994, in *Lecture Notes in Physics*, 428, 163
- Steffen, M., Szczerba, R., Schönberner, D. 1998, *A&A*, 337, 149
- Ueta, T., et al. 2006, *ApJ*, 648, L39
- Ueta, T., et al. 2007, in *AIP Conf. Ser.* 948 *Unsolved Problems in Stellar Physics: A Conference in Honor of Douglas Gough*, eds. R. J. Stanccliffe, G. Houdek, R. G., Martin, & C. A. Tout (AIP, New York), 365
- Wareing, C. J., Zijlstra, A. A., O’Brien, T. J., Seibert, M. 2007, *ApJ*, 670, L125
- Werner, M. W., et al. 2004, *ApJS*, 154, 1
- Zank, G. P. 1999, *Sp. Sci. Rev.* 89, 413

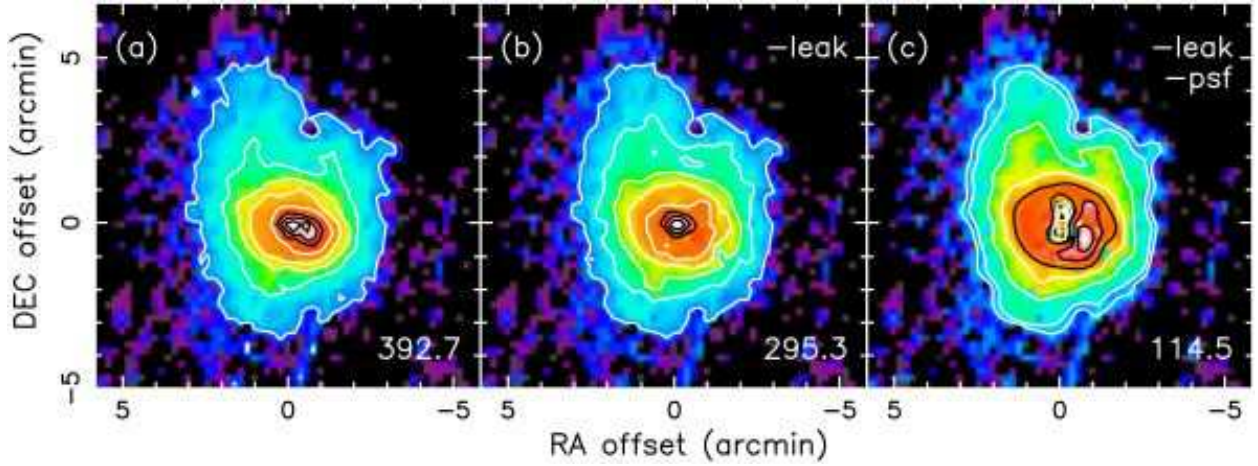


Fig. 1.— *Spitzer*/MIPS far-infrared image of Mira’s astropause at $160\mu\text{m}$. **(a)** Calibration-optimized, saturation-corrected image in the $12''\text{pixel}^{-1}$ scale (\square) centered at the position of Mira (north is up, east to the left) based on SWIRE/XMM-LSS scans, which yielded 1σ sensitivity of 0.8 MJy sr^{-1} . The contours represent 80, 60, 40, 20, 10, 5, 2.5 and 0.5% of the peak surface brightness, which is indicated at the bottom right corner in MJy sr^{-1} . The lowest contour corresponds to emission at 3σ level ($= 2.5\text{ MJy sr}^{-1}$). The extent of the detected ($> 3\sigma$) emission halo is $8'.5$ long and $6'.5$ wide roughly at the PA of 15° . **(b)** Same as (a), but for the short-wavelength light-leak removed image. The slightly-elongated, singly-peaked core ($> 40\%$ of the peak) is surrounded by the similarly elongated plateau ($> 5\%$ of the peak) at the PA of 70° . **(c)** Same as (b), but for the core-fitted-PSF subtracted image. The lowest contour is 2.5% of the peak. The plateau is not entirely due to PSF and there is a ring of emission (at $\sim 40\%$ of the peak; $2'.4 \times 2'.0$ at the PA of 70°).

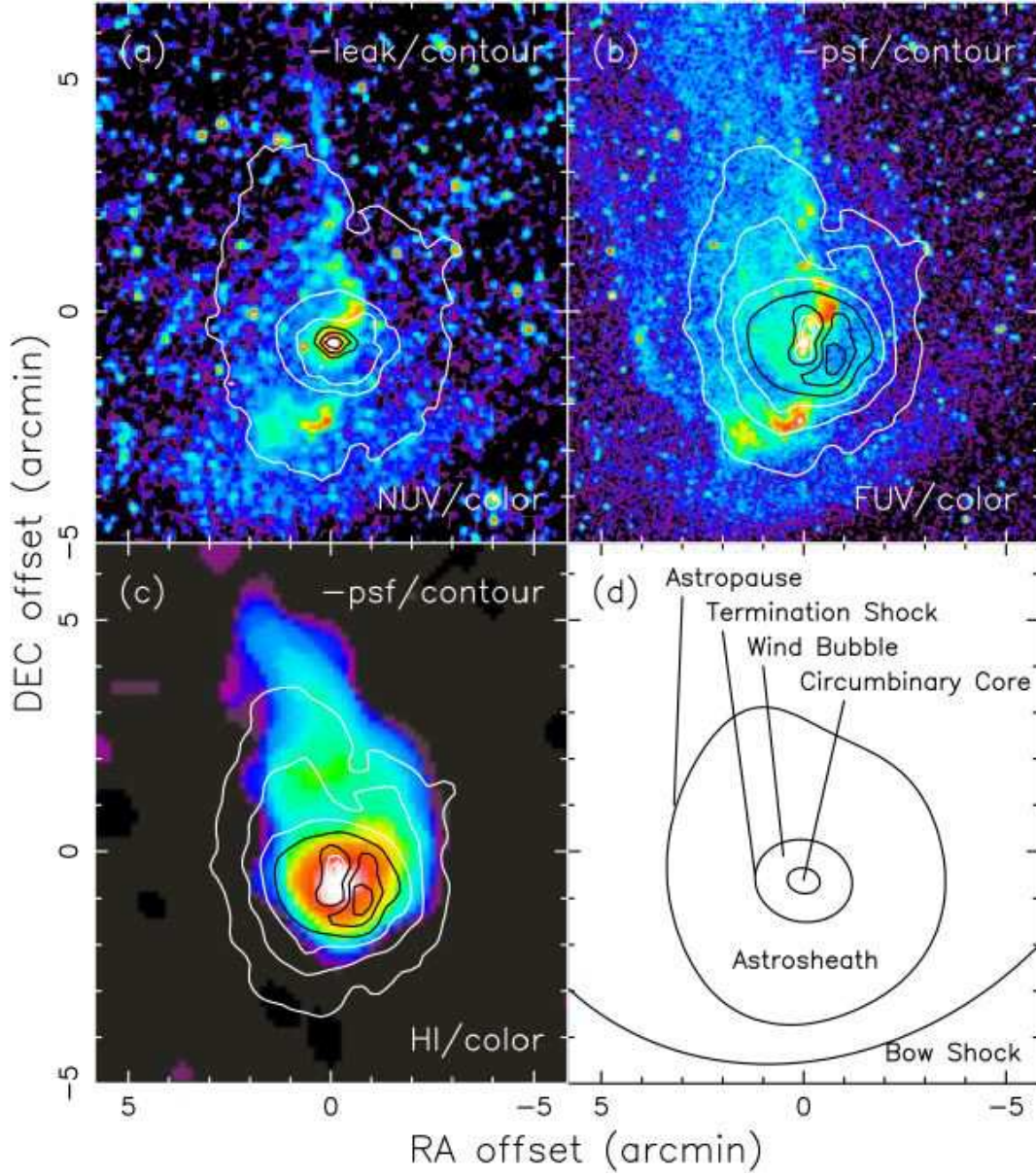


Fig. 2.— $\text{H}_2/\text{H I}$ imaging data overlaid with the $160\mu\text{m}$ contours of Mira’s astropause, and a schematic of its structure emerging from the present study. **(a)** Near-ultraviolet color image (Martin et al. 2007) overlaid with the leak-corrected $160\mu\text{m}$ contours, showing the spatial relationship between emission in these two bands. The contours represent 80, 60, 40, 20, 10, and 0.5% (3σ) of the peak surface brightness. **(b)** Same as (a), but far-ultraviolet color image (Martin et al. 2007) overlaid with the leak-corrected, core-subtracted $160\mu\text{m}$ contours. **(c)** Same as (a), but 21 cm H I color image (Matthews et al. 2008) overlaid with the leak-corrected, core-subtracted $160\mu\text{m}$ contours. **(d)** Schematic of the structure of Mira’s astropause revealed by the $160\mu\text{m}$ image and its spatial relationship with respect to $\text{H}_2/\text{H I}$ distribution. The circumbinary dust envelope, the termination shock and the astrosheath are spatially distinguished in the far-infrared for the first time.